

Supplementary Information

Magnetic Solid-Phase Extraction of Carbamate Pesticides Using Magnetic Metal–Organic Frameworks Derived from Benzoate Ligands, Followed by Digital Image Colorimetric Screening and High-Performance Liquid Chromatography Analysis

Jirasak Gamonchuang¹, Yanawath Santaladchaiyakit², Rodjana Burakham^{1*}

¹Materials Chemistry Research Center, Department of Chemistry, Faculty of Science, Khon Kaen University, Khon Kaen 40002, Thailand

²Department of Chemistry, Faculty of Engineering, Rajamangala University of Technology Isan, Khon Kaen Campus, Khon Kaen 40000, Thailand

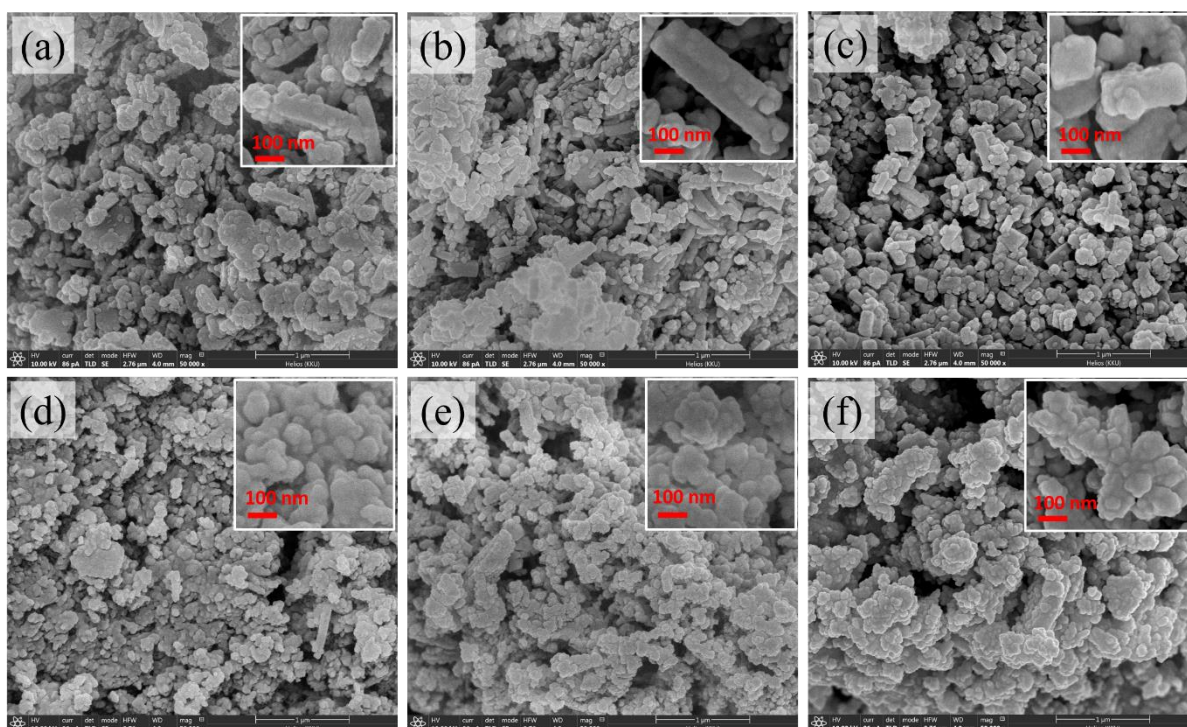


Figure S1. SEM images of (a) bare Fe-Al MMH, (b) Fe-Al MMH@MOF(Fe-H₂BDC), (c) Fe-Al MMH@MOF(Fe-H₂BDC-NH₂), (d) Fe-Al MMH@MOF(Fe-H₂BDC-DH), (e) Fe-Al MMH@MOF(Fe-H₃BTC), and (f) Fe-Al MMH@MOF(Fe-H₄BTtC).

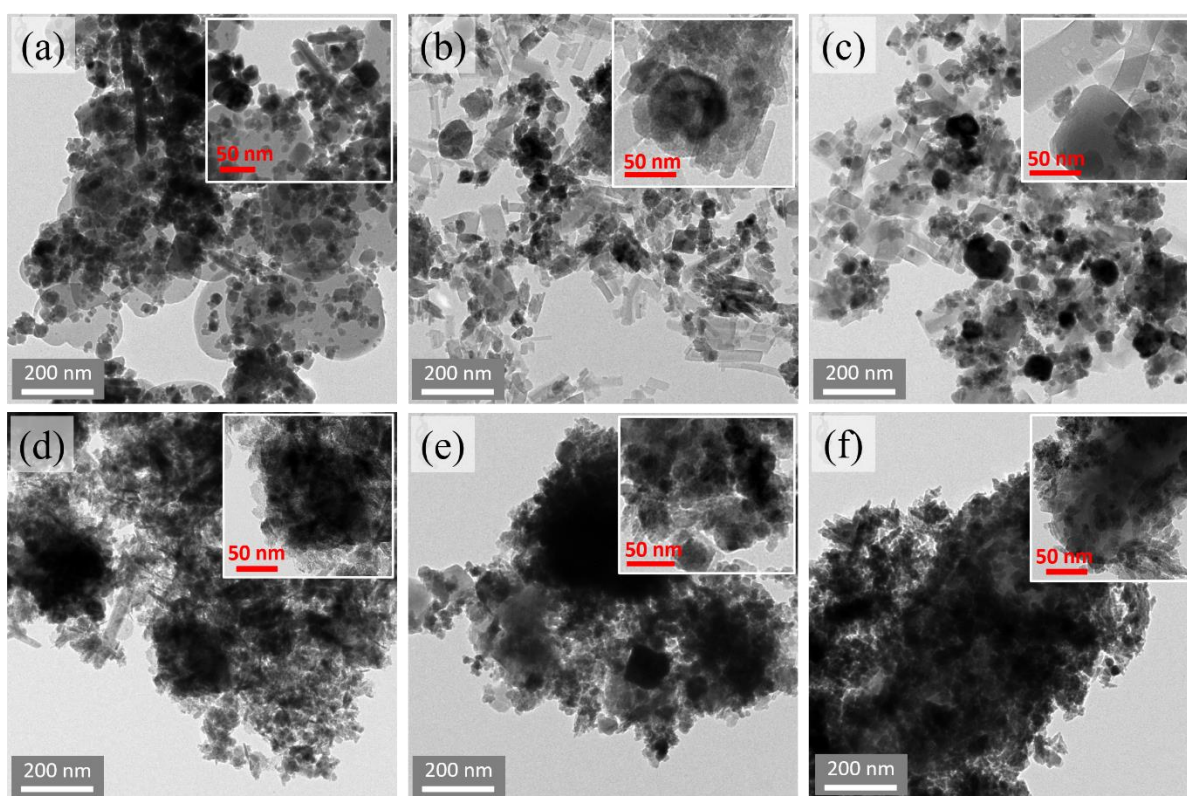


Figure S2. TEM images of (a) bare Fe-Al MMH, (b) Fe-Al MMH@MOF(Fe-H₂BDC), (c) Fe-Al MMH@MOF(Fe-H₂BDC-NH₂), (d) Fe-Al MMH@MOF(Fe-H₂BDC-DH), (e) Fe-Al MMH@MOF(Fe-H₃BTC), and (f) Fe-Al MMH@MOF(Fe-H₄BTtC).

TGA was performed at temperatures between 40–900 °C under a N₂ atmosphere. The TG curves of the bare Fe-Al MMH and Fe-Al MMH@MOF composites are illustrated in Figure S3. Two stages of thermal decomposition were observed for bare Fe-Al MMH. The first stage of weight loss (7 wt%) was found at temperatures between 40–290 °C, corresponding to the removal of water and DMF from inner and outer particles. The second stage appeared from 600 °C to 800 °C, indicating its phase transition. For Fe-Al MMH@MOF(Fe-H₂BDC) and Fe-Al MMH@MOF(Fe-H₂BDC-NH₂), weight loss was found from 40 °C to 290 °C, and was attributed to the decomposition of water and DMF (Figure S3(b, c)). The weight losses of approximately 27 wt% (350–570 °C) and 14 wt% (350–570 °C) were due to the decomposition of the framework and removal of H₂BDC and H₂BDC-NH₂ ligands, respectively. The final stage of weight loss (16 wt%) was observed in the range of 700–840 °C due to the decomposition of the H₂BDC-NH₂ ligand. In Figure S3(d–f), the first stage of mass conversion was observed from 40 to 100 °C, corresponding to dehydration on the surface. Thermal decomposition of MMOF was found between 200–520 °C. Weight losses of approximately 18 wt%, 28 wt% and 27 wt% were suggested for the removal of H₂BDC-DH, H₃BTC and H₄BTtC ligands from MMOF, respectively. These results confirmed the existence of a composite material between Fe-Al MMH and MOFs.²³⁻

24, 27–29

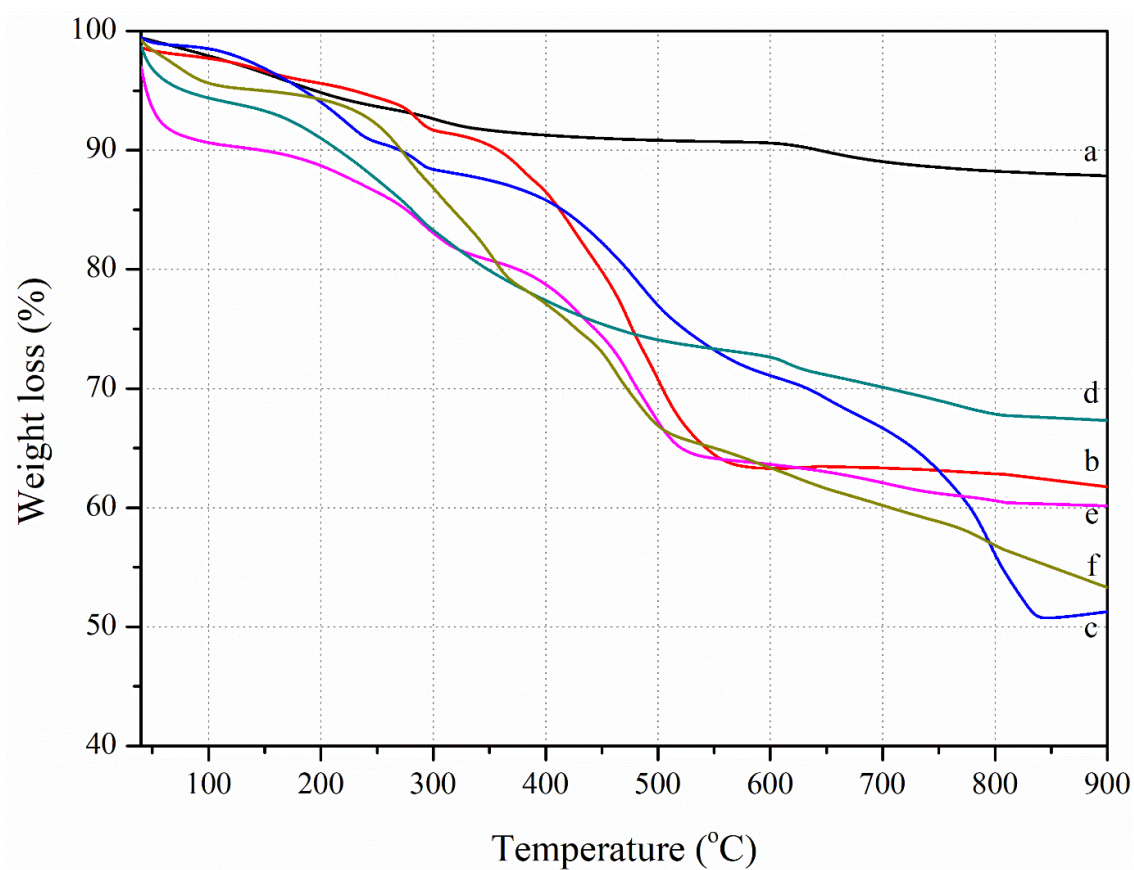


Figure S3. TG curves of (a) bare Fe-Al MMH, (b) Fe-Al MMH@MOF(Fe-H₂BDC), (c) Fe-Al MMH@MOF(Fe-H₂BDC-NH₂), (d) Fe-Al MMH@MOF(Fe-H₂BDC-DH), (e) Fe-Al MMH@MOF(Fe-H₃BTC), and (f) Fe-Al MMH@MOF(Fe-H₄BTiC).

The magnetic properties of the as-prepared sorbents were measured, as shown in Figure S4. The appearances of the hysteresis, remanence, and coercivity values demonstrated that all magnetic sorbents were ferromagnetic materials. The saturated magnetization of bare Fe-Al MMH was approximately 40.3 emu g^{-1} , while the composite materials attained values of 15.4, 31.0, 16.0, 32.5, and 14.0 emu g^{-1} for Fe-Al MMH@MOF(Fe-H₂BDC), Fe-Al MMH@MOF(Fe-H₂BDC-NH₂), Fe-Al MMH@MOF(Fe-H₂BDC-DH), Fe-Al MMH@MOF(Fe-H₃BTC), and Fe-Al MMH@MOF(Fe-H₄BTtC), respectively. The presence of paramagnetic MOFs resulted in a decrease in the magnetization values of the synthesized composites. In the MSPE procedure, however, it was sufficient for complete phase isolation within 1 min.

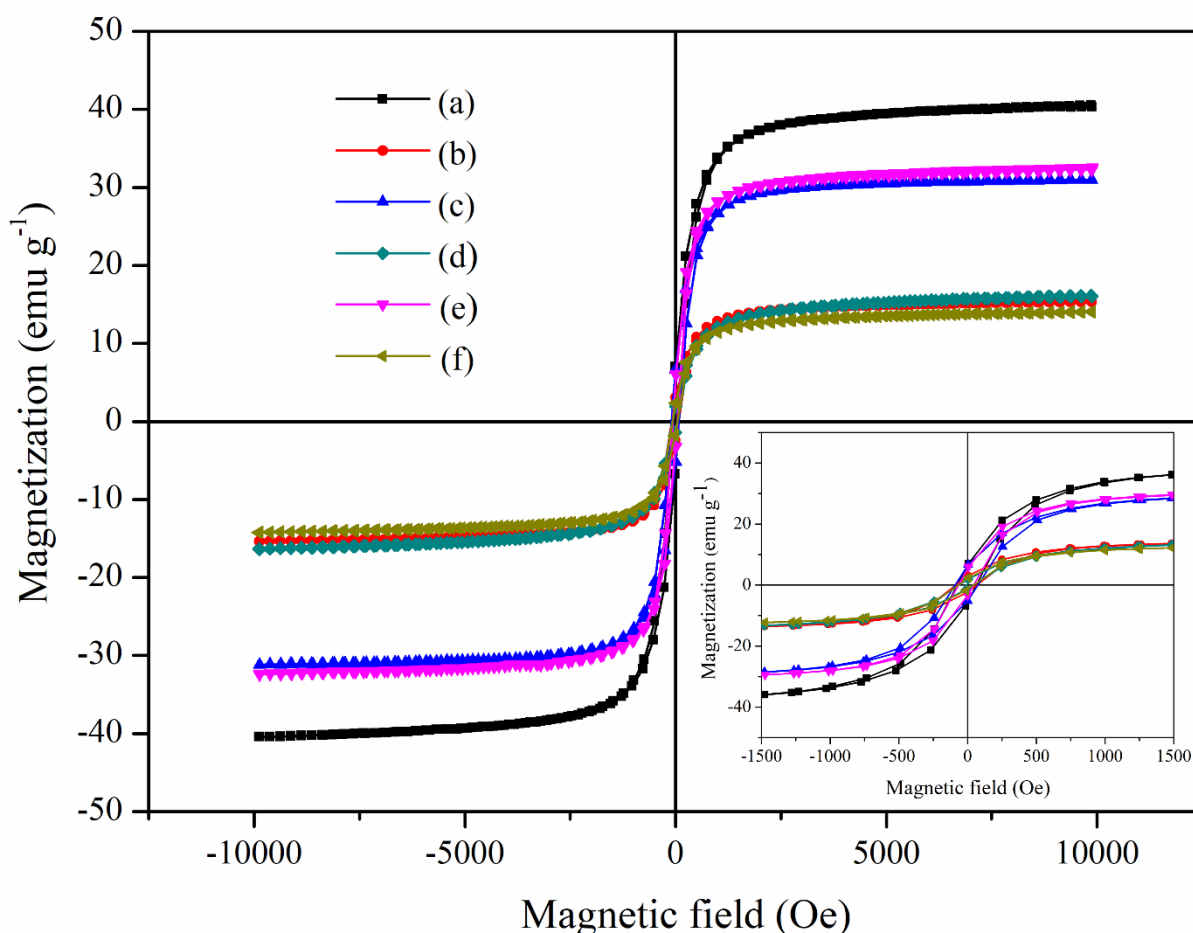


Figure S4. Magnetic properties of (a) bare Fe-Al MMH, (b) Fe-Al MMH@MOF(Fe-H₂BDC), (c) Fe-Al MMH@MOF(Fe-H₂BDC-NH₂), (d) Fe-Al MMH@MOF(Fe-H₂BDC-DH), (e) Fe-Al MMH@MOF(Fe-H₃BTC), and (f) Fe-Al MMH@MOF(Fe-H₄BTtC).

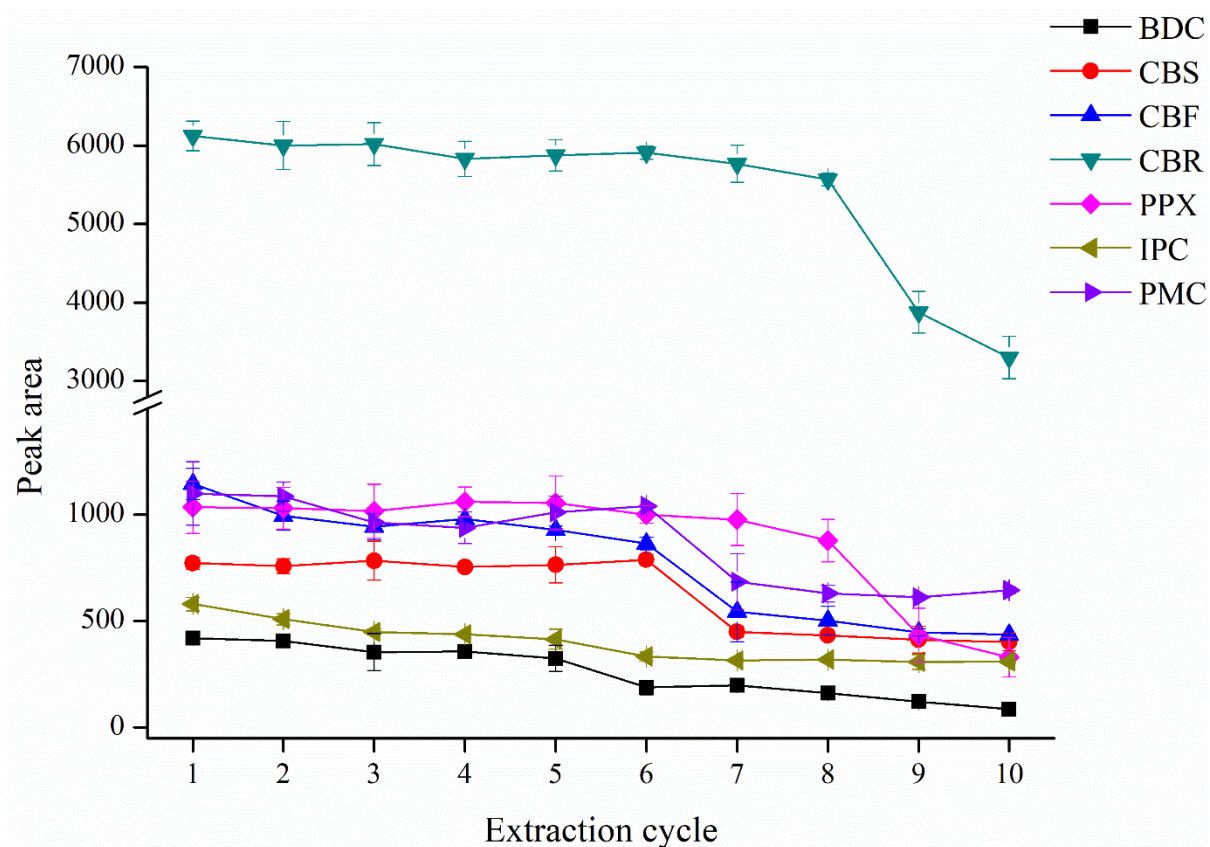


Figure S5. Reusability of the Fe-Al MMH@MOF(Fe-H₂BDC) sorbent.

Table S1. Analytical performance of the proposed MSPE coupled with digital image colorimetry.

Analyte	Linear range ($\mu\text{g L}^{-1}$)	Linear equation	R^2	RSD (%)		DI water		Long bean		Orange	
				Intraday	Interday	LOD	LOQ	LOD	LOQ	LOD	LOQ
				(n=5)	(n=5 \times 3)	($\mu\text{g L}^{-1}$)	($\mu\text{g L}^{-1}$)	($\mu\text{g L}^{-1}$)	($\mu\text{g L}^{-1}$)	($\mu\text{g L}^{-1}$)	($\mu\text{g L}^{-1}$)
BDC	60.0–500.0	$y = 0.53x + 6.40$	0.9982	7.9	9.8	18.0	60.0	20.0	60.0	20.0	60.0
CBS	26.0–300.0	$y = 0.12x + 3.00$	0.9832	3.1	9.0	8.0	26.0	15.0	40.0	15.0	40.0
CBF	30.0–500.0	$y = 0.10x + 5.40$	0.9994	3.4	6.9	9.5	30.0	15.0	40.0	15.0	40.0
CBR	6.0–100.0	$y = 0.53x + 2.90$	0.9981	0.4	1.2	2.0	6.0	3.0	10.0	4.0	12.0
PPX	8.0–100.0	$y = 0.37x + 8.00$	0.9903	7.3	8.1	2.5	8.0	5.0	15.0	5.0	15.0
IPC	7.0–100.0	$y = 0.47x + 6.50$	0.9874	4.2	6.5	2.0	7.0	10.0	30.0	10.0	30.0
PMC	9.0–100.0	$y = 0.35x + 9.00$	0.9887	0.5	1.3	3.0	9.0	10.0	30.0	10.0	30.0
Mixed (7 carbamates)	3.0–100.0	$y = 0.92x + 11.00$	0.9638	1.6	7.3	1.0	3.0	1.0	3.0	1.0	3.0

Table S2. Sorption capacity of the studied magnetic sorbents

Sorbent	Q_{\max} (mg kg ⁻¹)						
	BDC	CBS	CBF	CBR	PPX	IPC	PMC
Fe-Al MMH	1435	1141	759	486	466	2714	1871
Fe-Al MMH@MOF(Fe-H ₂ BDC) ^a	3343	3200	2823	2993	2193	3327	4196
Fe-Al MMH@MOF(Fe-H ₂ BDC) ^b	3193	3176	2750	2978	2037	3096	4116
Fe-Al MMH@MOF(Fe-H ₂ BDC) ^c	3018	3115	2690	2907	1984	3015	3925
Fe-Al MMH@MOF(Fe-H ₂ BDC-NH ₂)	1949	2908	2638	2815	2110	3160	3808
Fe-Al MMH@MOF(Fe-H ₂ BDC-DH)	1016	1321	948	1205	1144	1866	2034
Fe-Al MMH@MOF(Fe-H ₃ BTC)	1352	1424	964	1249	1362	1434	2090
Fe-Al MMH@MOF(Fe-H ₄ BTtC)	1110	1458	1127	1102	534	3202	2163

^a Evaluated in DI water.

^b Evaluated in long bean extract.

^c Evaluated in orange extract.

Table S3. Comparison of the proposed MSPE method with other methods based on MMOF sorbents for carbamate determination.

Magnetic sorbent ^{Ref.}	Analytes	Sample matrix	Analysis method	Analytical performance
Zn/Co-MOF-5 ¹⁵	Methomyl, 3-hydroxycarbofuran, CBF, IPC	Drinking water and tomato	HPLC-MS/MS	Linear range: 0.05–20 ng mL ⁻¹ , 0.1–40 ng g ⁻¹ LODs: 0.0006–0.013 ng mL ⁻¹ , 0.001–0.01 ng g ⁻¹ RSDs: < 14% %R: 86.1–109.1 Reusability: Not reported Q_{\max} : 63.22–87.33 mg g ⁻¹ EF: Not reported
Magnetic porous covalent triazine-based organic polymer (M-PCTP) ¹⁶	PPX, CBR, IPC, fenobucarb, and diethofencarb	Lemonade and grape juice	HPLC-MS	Linear range: 0.06–80 ng mL ⁻¹ LODs: 0.02–0.3 ng mL ⁻¹ LOQs: 0.06–0.9 ng mL ⁻¹ RSDs: < 6.2% %R: 86.3–108.0 Reusability: 20 cycles Q_{\max} : Not reported EF: Not reported
Fe ₃ O ₄ -doped porous carbon (MPC) ²²	PPX, CBR, IPC, and fenobucarb	Apple	HPLC-UV	Linear range: 1–100 ng g ⁻¹ LOQs: 0.1–0.2 ng g ⁻¹ RSDs: < 5.7% %R: 89.3–109.7 Reusability: 13 cycles Q_{\max} : Not reported EF: Not reported
Fe-Al MMH@MOF(Fe-H ₂ BDC) ^{This study}	BDC, CBS, CBF, CBR, PPX, IPC, and PMC	Guava, pomelo, pineapple, watermelon, orange, mango, grape, long bean, and Chinese cabbage	Digital image colorimetry and HPLC-UV	Linear range: 0.015–1000 µg L ⁻¹ LODs: 0.005–0.09 µg L ⁻¹ LOQs: 0.015–0.3 µg L ⁻¹ RSDs: <10.7% %R: 74.9–122.7 Reusability: 8 cycles Q_{\max} : 2823–4196 mg kg ⁻¹ EF: 29–184